Fate of the superradiant mode in a resonant Bragg reflector

Tomoe Ikawa* and Kikuo Cho†
Graduate School of Engineering Science, Osaka University, Toyonaka, 560-8531 Japan
(Received 23 October 2001; revised manuscript received 07 March 2002; published 30 August 2002)

Based on the first-principles theory of radiative correction, it is demonstrated that the well-known superradiant (SR) mode in a resonant Bragg reflector consisting of N layers loses its meaning when the frequency dependence of its radiative width becomes no longer negligible within its spectral width in the course of increasing N. Beyond this range of N, it evolves, together with a part of subradiant modes, into the states forming the light-reflecting photonic gap. On the other hand, the rest of the subradiant modes form very narrow light-transmitting modes in the gap region. This conclusion is reached by calculating the N dependence of the reflectance in frequency and time domains with the explicit consideration of a frequency-dependent radiative shift and width. The intrinsic limit of the speedup effect of the radiative decay of the SR mode is given for various cases.

DOI: 10.1103/PhysRevB.66.085338 PACS number(s): 78.67.De, 42.70.Qs, 78.47.+p, 42.50.−p

I. INTRODUCTION

The radiation-matter interaction is generally enhanced in a resonant condition where the light frequency is in resonance with an excitation energy of the matter. For an array of N_r units of a resonant matter in a space smaller than the resonant wavelength, there is an additional enhancement of the coupling with light for a mode which almost monopolizes the coupling strength. Such a mode is possible for a one-dimensional (1D) chain and a 2D plane and called ''superradiant'' (SR).[1–3] The oscillator strength of this mode is propotional to N_r, as long as the linear extension of the array is smaller than the resonant wavelength. For a chain or a plane with infinite extension, there is a group of radiative modes which arises from the saturated SR mode. The radiative modes have lateral wave number $k_\parallel \leqslant \omega/c$, and, on average, each one of them has the coupling strength with light $(\lambda_r/2b)^D$ times that of a single resonant unit. Here, b is the lattice constant of the arrays (chain or plane) and $D=1$ and 2 for the chain and plane, respectively. This enhanced coupling strength corresponds to the saturation value of the SR mode as one increases the size of N_r beyond the resonant wavelength.[3]

There is a different way to enhance the radiation-matter interaction. Namely, let us consider a set of identical N planes, each of which contains radiative modes (saturated SR modes) as mentioned above, and make an equidistant 1D array of them with lattice period $=\lambda_r/2$, which is a Bragg condition for resonant light. This kind of system is called a resonant Bragg reflector, where a further increase in the coupling strength occurs for a special combination of ''saturated SR modes.'' Noting that a saturated SR mode is already enhanced by the factor $F_{sat}=(\lambda_r/2b)^2$, we might better call the new combination of the saturated SR modes (for $N\geqslant 2$) something like the ''super SR'' mode. This naming will make sense to stress that it is the consequence of the two independent mechanisms of enhancement. However, we will use the terminology ''SR mode'' in the following, considering that it is widely used in the literature.

The observable feature of the enhanced interaction with light is either the enhanced radiative decay rate of the excited level or the large radiative width in the frequency domain. The former was discovered in the nuclear Bragg reflection as a speedup effect of the decay rate of the excited ^{57}Fe in enriched $FeBO_3$ by using synchrotron radiation for Mössbauer spectroscopy.[4] Later the experiments on multiple (N) quantum wells (QW's) showed the enhanced decay rate of superradiance by the factor of N in the time domain[5,6] or the N-linear broadening of reflectance spectrum in the frequency domain.[7–9]

Theoretical studies showed that, in multiple-quantum-well systems, strong light-induced interwell coupling occurs when the QW's are arranged with a spacing which satisfies the Bragg condition.[10,11] The enhancement factor for the SR mode was studied by Ivchenko *et al.* for a system of N QW's (Ref. 10) by means of the transfer matrix method. The reflection amplitude for frequency ω was shown to be $r_N(\omega) = -iN\Gamma_0/[\hbar\omega_0-\hbar\omega-i(\Gamma+N\Gamma_0)]$, where Γ_0 and Γ are the radiative and nonradiative widths, respectively, of a single QW. This expression shows that the whole system looks like a single oscillator with the radiative width $N\Gamma_0$. Namely, the SR mode completely monopolizes the coupling with the radiation field. All the other modes have no coupling with light.

In the case of a QW system, we can experimentally study the dependence of the radiative width (or decay rate) on the size of the system, i.e., the number N of QW's forming the Bragg reflector. The theory by Ivchenko *et al.* indicates that the radiative width of the superradiant mode increases linearly with N without limit. Though the linear increase in the small-N region is reasonable, the absence of the growth limit is of course unphysical, because an excited state of a matter with infinite radiative width would mean an indefinite level position. Moreover, the system with infinitely large N would correspond to a photonic crystal with the photonic gap at the very position of the resonant level, where a mode with an infinitely large radiative width cannot be located. Though the model with a single resonance treated by Ivchenko *et al.* is very much simplified, the consistency of quantum mechanics should lead to a more reasonable result about the N dependence. In spite of the strong interest in QW systems in recent publications, no work has clarified the fate of the superradi-

ant mode as one increases N, and a consistent picture of this evolution with photonic band formation has not been obtained. The purpose of this paper is to examine this very fundamental point of the problem, though the current interest in the study of QW systems seems to be attracted to the effects of inhomogeneity.[12–14].

The specific feature of the present study is that we calculate the radiative correction of the superradiant mode directly from first principles as a function of frequency. The explicit definition and evaluation of the radiative correction is a central point of the nonlocal theory of optical response,[15] which is applicable to arbitrary systems from an atom to bulk materials. This scheme is a generalization of the one for slab geometry[16] to arbitary systems of size and shape, and has been applied to studies of the size dependence of the optical response of mesoscopic systems beyond the long-wavelength approximation.[3,17,18] Similar schemes to describe the optical response in terms of the radiative correction were adopted later by Andreani *et al.*[20] and Citrin[21] for the study of single-QW systems. The radiative self-energy used by Citrin for a QW system is a special case of the radiative correction term given below.

In the scheme of the nonlocal response,[15] the finite extension of the matter wave functions, being the source of nonlocality, is explicitly taken into account, and the response field and the induced polarization are determined self-consistently for a given initial condition of matter and radiation. In doing so, the interaction among the components of induced polarization via a transverse electromagnetic (EM) field is explicitly taken into account. This is the retarded interaction, or radiative correction, among the induced polarizations, through which the matter excitation energies acquire radiative shifts and widths in optical response spectra. The radiative correction in this framework is defined in a straightforward way. Namely, it is the interaction energy between the components of the induced current density (or polarization) via a transverse (i.e., vacuum) EM field. Because the interaction is mediated by photons, it is *frequency dependent* by definition.

Usually, the radiative correction is a small effect, so that its frequency dependence is safely neglected, which allows us to assign its real and imaginary parts to the radiative shift and width, respectively, of the relevant transition energy. However, a resonant Bragg reflector with arbitrary size N is an *exceptional* optical medium, in the sense that it contains an automatic mechanism to break the frequency independence of the radiative correction. Namely, the radiative correction grows so much with N that its frequency dependence can eventually no longer be negligible within its spectral width. Though the frequency dependence of the radiative correction may be encountered in various other problems, the present example will be a most dramatic one. This is the reason why we concentrate our discussion on this particular example. The importance of the frequency dependence was noted in our previous study of resonant Bragg reflectors,[22] and this paper gives a full description of this subject. A brief report of this work was given in a conference proceedings.[23]

If one considers the frequency dependence in the transfer matrix method correctly, the calculated reflectance curve with a Lorentzian shape for small N (SR mode behavior) evolves into a silk-hat shape (photonic band behavior) as N increases. However, this does not mean that the physical meaning of the evolution is understood. This is because the transfer matrix method is just a mathematical tool applicable to many different physical problems. On the other hand, the scheme of the microscopic nonlocal response describes optical processes in terms of the quantities with clear physical meaning such as resonant energies, current density, radiative shift and width, etc. This allows us an appropriate interpretation of the spectral evolution from the SR mode to photonic band behavior as due to the fact that the frequency dependence of the radiative correction, negligible for small N, becomes too large to be neglected as N gets larger. The two approaches give the same spectral behavior, but the physical meaning is more easily obtained by one of them. On the other hand, we can compare the two schemes, not numerically, but analytically. Starting from the solution of a single-layer problem in the nonlocal scheme to fix the elements of the transfer matrix, we try to rewrite the field equations of the transfer matrix method for the N-layer problem into those of the nonlocal scheme. We have been able to demonstrate the analytical equivalence in this manner. But the transfer matrix elements we obtained are somewhat different from those of Ivchenko *et al.*[10] The difference is negligible if the thickness of the resonant layer is much less than the resonant wavelength. This result will be published elsewhere.[24]

In terms of the frequency dependence of the radiative correction, we can establish a consistent picture of ''the evolution from the SR mode for small N to the photonic gap for large N'' within a single theoretical framework. The evolution appears in the reflectivity spectrum as that from a Lorentzian to a silk-hat form and also in the temporal decay of the reflected light for a short-pulse incidence. The explicit evaluation of the radiative correction for the SR mode shows the importance of the frequency dependence beyond a certain range of N, where the optical response is no longer represented solely by the SR mode. It should be noted that, in spite of the drastic spectral evolution, the strongly light-reflecting character of the system is kept preserved, indicating the strong coupling of the Bragg arrangement of the resonant levels. On the other hand, a tiny left over of the monopolized radiation-matter coupling due to the SR mode is distributed among the non radiant modes. These modes show themselves in the reflectance spectrum as very thin dips in the total reflection range for a finite-N system. This group of levels evolves into the gap mode branch in the limit of the photonic crystal ($N=\infty$).

The criterion for the existence of the SR mode is the negligibility of the frequency dependence of the radiative correction of this mode. The dependence will be shown explicitly, but a rough criterion for the linear growth of the radiative width of the SR mode will be that the width is much less than the photonic gap E_{gap}. This criterion will be tested later for some model systems with reasonable success.

This evolution requires a corresponding change in the concept of the coupled modes of a radiation-matter system. When the radiative correction is frequency independent, the coupled modes are the modified matter excitations corrected

with a certain radiative width and shift. As for the number of the degrees of freedom, only those of the matter excitations are relevant as coupled modes. When the frequency dependence of the radiative correction is important, however, the radiation degrees of freedom become also important in describing the eigenmodes of the coupled radiation-matter system. This is typically exemplified by the eigenmodes of the $N\rightarrow\infty$ limit of a resonant Bragg reflector, where the eigenmodes are the photonic band states.[25–27]

In connection with the fate of the SR mode for increasing N, there is an additional problem about the photonic band dispersion for $N\rightarrow\infty$: A commonly accepted dispersion equation in the literature,[28–30] obtained from a Kronig-Penny-type treatment, has the following form for the frequency ω and wave number k:

$$\cos kd=\cos qd-\Gamma_0\frac{\sin qd}{\omega_0-\omega-i\gamma}, \tag{1}$$

where $q=\omega/c$, ω_0 is the resonant frequency, γ the nonradiative decay constant, and Γ_0 the radiative width of a single QW. In the neighborhood of the lowest photonic gap, this equation has three branches in general, which contain a flat-band representing the resonant levels. At the exact Bragg condition $\omega_0=\pi c/d$ and for vanishing γ, however, the resonant (gap) mode arising from the energy denominator disappears. This is because $\sin qd/(\omega_0-\omega)=\sin[\pi(\omega_0-\omega)/\omega_0]/(\omega_0-\omega)$ does not contain resonant character any more. This result is not physically reasonable, because the nonradiative damping may affect the form but not the *number* of dispersion curves. Namely, the gap mode should exist even in an idealized situation of vanishing nonradiative damping. Thus the question is why the above equation leads to such a result and how one can obtain more reasonable dispersion curves.

Here also the nonlocal framework works well as an appropriate tool. Applying it to an arbitrary periodic system, we obtain a dispersion equation of the coupled radiation-matter system from the condition for the existence of a nontrivial solution in the absence of an external field. This is a generalized polariton dispersion equation including the effect of Bragg scattering,[25] or it is an advanced version of the x-ray dynamical scattering scheme[31] including the effect of resonant levels. Using this scheme for the 1D resonant Bragg reflector with a single resonant level, we obtain a simple dispersion equation for the photonic bands. This equation leads to the three branch dispersion curves in the lowest-gap region.[32] Two of them are the usual branches of photonic bands on both sides of the gap, and the very flat third branch in the gap is the mode due to the resonant levels of the matter. All of them have real wave number for real frequency. As evidence of this mode, we have found a series of ultrasharp dips in the total reflection range of the reflectance spectrum of finite-N systems. The positions of these dips lie within the dispersion of the gap mode, and the induced internal fields at these frequencies have standing-wave patterns, reflecting the propagating wave nature of the gap mode.

II. RADIATIVE WIDTH AND SHIFT

First of all, let us define the matter and EM field precisely. We take the Coulomb gauge and include the full Coulomb interaction among the charged particles in the matter Hamiltonian, leaving only the transverse modes as the radiation field.

According to the nonlocal response theory, the matter is represented by various components of the induced current density, interacting with the vector potential of the EM field. Each component of the current density is an electric oscillator with its specific spatial extension. Its eigenfrequency corresponds to a transition energy of the matter system, which may contain a nonradiative width. When these oscillators interact with the EM field, they undergo forced oscillations. This produces an additional radiation field, which further interacts with the oscillators, and so on. In this way, the oscillators interact with one another via the radiation field, through which their eigenfrequencies get shifted and broadened.

The radiative correction is the interaction among the components of the induced current density (or polarization) via the transverse EM field. Its matrix element between the two components of the current density associated with the transitions $\mu\rightarrow\nu$ and $\sigma\rightarrow\tau$ is given as

$$\tilde{\mathcal{A}}_{\mu\nu,\tau\sigma}(\omega)=-\frac{1}{c}\int d\boldsymbol{r}\boldsymbol{I}_{\mu\nu}(\boldsymbol{r})\cdot\boldsymbol{A}_{\tau\sigma}(\boldsymbol{r},\omega), \tag{2}$$

where $\boldsymbol{A}_{\tau\sigma}(\boldsymbol{r},\omega)$ is the vector potential at $\boldsymbol{r}$ produced by the (source) curent density $\boldsymbol{I}_{\tau\sigma}$ via the EM field with frequency ω. This induced field is obtained from the Maxwell equation as

$$\boldsymbol{A}_{\tau\sigma}(\boldsymbol{r},\omega)=\frac{1}{c}\int d\boldsymbol{r}'\tilde{\mathbf{G}}_q(\boldsymbol{r},\boldsymbol{r}';\omega)\cdot\boldsymbol{I}_{\tau\sigma}(\boldsymbol{r}')\quad\left(q=\frac{\omega}{c}\right). \tag{3}$$

The transverse EM Green's function $\tilde{\mathbf{G}}_q$ is given in Fourier representation as

$$\tilde{\mathbf{G}}_q(\boldsymbol{r},\boldsymbol{r}',\omega)=\frac{1}{2\pi^2}\int d\boldsymbol{k}\frac{e^{i\mathbf{k}\cdot(\mathbf{r}-\mathbf{r}')}}{k^2-(q+i0^+)^2}(\mathbf{1}-\hat{\boldsymbol{e}}_{\mathbf{k}}\hat{\boldsymbol{e}}_{\mathbf{k}}), \tag{4}$$

where $\hat{\boldsymbol{e}}_{\mathbf{k}}$ is the unit vector in the direction of $\boldsymbol{k}$. Thus the radiative correction can be written as

$$\tilde{\mathcal{A}}_{\mu\nu,\tau\sigma}(\omega)=-\frac{1}{2\pi^2c^2}\int d\boldsymbol{k}\frac{1}{k^2-(q+i0^+)^2}\times\tilde{\boldsymbol{I}}_{\mu\nu}(-\boldsymbol{k})\cdot(\mathbf{1}-\hat{\boldsymbol{e}}_{\mathbf{k}}\hat{\boldsymbol{e}}_{\mathbf{k}})\cdot\tilde{\boldsymbol{I}}_{\tau\sigma}(\boldsymbol{k}), \tag{5}$$

where

$$\tilde{\boldsymbol{I}}_{\tau\sigma}(\boldsymbol{k})=\int d\boldsymbol{r}\,e^{-i\mathbf{k}\cdot\mathbf{r}}\boldsymbol{I}_{\tau\sigma}(\boldsymbol{r}). \tag{6}$$

For each given model, we only need to evaluate the current density and carry out the integration.

In the framework of nonlocal response theory, the radiative correction $\tilde{\mathcal{A}}_{\mu\nu,\tau\sigma}$ plays an essential role in determining

the response of matter and field. The part of the framework relevant to this work is the linear response of a small number of resonant levels. The effect of nonresonant levels will be taken into account as background susceptibility, if necessary. The resonant part of the induced current density is given as

$$\boldsymbol{J}(\boldsymbol{r},\omega)=\frac{1}{c}\sum_{\nu}{}' \, g_{\nu}(\omega)F_{\nu 0}(\omega)\boldsymbol{I}_{0\nu}(\boldsymbol{r}), \tag{7}$$

where the summation over ν is restricted to resonant levels and the factor $\{g_{\nu}\}$ is defined as

$$g_{\nu}=\frac{1}{E_{\nu 0}-\hbar\omega-i0^{+}}. \tag{8}$$

Here $E_{\nu 0}$ is the νth excitation energy of the matter from its ground state. The factors

$$F_{\nu 0}(\omega)=\int d\boldsymbol{r}\boldsymbol{I}_{\nu 0}(\boldsymbol{r})\cdot\boldsymbol{A}(\boldsymbol{r},\omega) \tag{9}$$

contain the vector potential to be determined. The vector potential produced by $\boldsymbol{J}(\boldsymbol{r},\omega)$ is calculated via Eq. (3) above by replacing $\boldsymbol{I}_{\tau\sigma}(\boldsymbol{r}')$ by $\boldsymbol{J}(\boldsymbol{r}',\omega)$. In the Fourier representation, we have

$$\boldsymbol{A}(\boldsymbol{r},\omega)=\boldsymbol{A}_0(\boldsymbol{r},\omega)+\frac{1}{2\pi^2c^2}\int d\boldsymbol{k}\frac{g_{\nu}(\omega)F_{\nu 0}(\omega)\tilde{\boldsymbol{I}}_{0\nu}(-\boldsymbol{k})e^{i\mathbf{k}\cdot\mathbf{r}}}{k^2-(q+i0^{+})^2}, \tag{10}$$

where $\boldsymbol{A}_0$ represents the incident field. The equations to determine $\{F_{\mu 0}\}$ self-consistently are[15,17] (Ref. 33)

$$F^{(0)}_{\mu 0}=\sum_{\nu}\{(E_{\nu 0}-\hbar\omega)\delta_{\mu\nu}+\tilde{\mathcal{A}}_{\mu 0,0\nu}\}g_{\nu}F_{\nu 0}, \tag{11}$$

where $F^{(0)}_{\mu 0}$ is defined as Eq. (9) with $\boldsymbol{A}$ replaced with the incident field $\boldsymbol{A}_0$. Equation (11) may be written in the form of a matrix equation

$$\mathbf{SX}=\mathbf{F}^{(0)}, \tag{12}$$

where $X_{\mu}=g_{\mu}F_{\mu 0}$ and $\mathbf{S}$ is the coefficient matrix.

Without the radiative correction, the solution is just $F_{\mu 0}=F^{(0)}_{\mu 0}$. Namely, all the oscillators respond independently to the incident EM field. The radiative correction terms mix the oscillator states in such a way that they acquire different resonance energies and also radiative widths.

The radiative correction is a general measure of the coupling strength.[27] If it is small compared with the interval of the matter excitation energies, as in atoms, we may treat it perturbationally. Namely, for each resonance at $E_{\nu 0}$, $\tilde{\mathcal{A}}_{\nu 0,0\nu}(\omega)$ is replaced by $\tilde{\mathcal{A}}_{\nu 0,0\nu}(\omega=E_{\nu 0}/\hbar)$, the real and imaginary parts of which give the radiative shift and width of the excitation energy $E_{\nu 0}$.

In mesoscopic systems, the energy separation of matter-excited states becomes small and can be comparable to the radiative shift or width, so that a careful treatment is necessary about the radiative correction. We should not neglect either the off-diagonal elements or the ω dependence. The case of a SR mode is rather extreme in the sense that the ω dependenc of $\tilde{\mathcal{A}}$ can change the qualitative structure of the problem as will be discussed below.

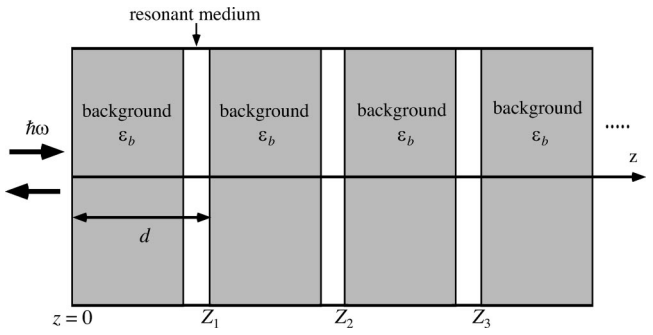

FIG. 1. Geometry of light reflection for the two models. For model (A), $\varepsilon_b=1$, $d=\lambda_r/2$.

The eigenmodes of the system in the presence of the radiative corection are derived from the condition $\det|\mathbf{S}|=0$. Since these are nontrivial solutions in the absence of an external field, we may call them self-sustaining (SS) modes. This equation is quite useful to see the detailed spectral structure of any coupled radiation-matter system. It will be used later to derive the dispersion equation of the photonic crystal.

Though the above scheme can always be used for calculation of the optical response, the characterization of the SS modes is strongly affected by the ω dependence of $\tilde{\mathcal{A}}$. If one can neglect the ω dependence, we obtain N' SS modes for a set of N' excited states of matter, because $\det|\mathbf{S}|=0$ is a polynomial equation of the N'th order. However, if the ω dependence of $\tilde{\mathcal{A}}$ is important, $\det|\mathbf{S}|=0$ is no longer a polynomial equation of the N'th order. Then, the physical picture of its solution is no longer simple. This situation is the case in the evolution of the resonant Bragg reflector for larger N.

III. MODEL AND NUMERICAL CALCULATION

We consider two models of the 1D resonant Bragg reflector, i.e., the regular arrays in the z direction of (A) N single planes of H atoms and (B) N quantum wells, with lattice constant d equal to one-half the resonant wavelength λ_r (Fig. 1). The atomic plane is assumed to be a square lattice with lattice constant b. Both b and the lateral lattice constant of the QW are assumed to be much smaller than d. Then, the Bragg scattering of near-resonant light involves only the reciprocal lattice vectors in the normal (z) direction. The incident field is assumed to be normal to the atomic planes and QW's. Then, we only need to consider states with vanishing lateral wave vector ($\boldsymbol{k}_{\parallel}=0$) for both matter and field.

Model (A) is a fictitious one consisting of single two-level atoms, to which the framework of Sec. II directly applies with the restriction of the level indices $(0,\nu)$ to those of the two-levels ($1s$ and $2p$). We neglect all nonresonant levels, which may contribute to the background polarization. The effect of background polarization is taken into account in model (B), as well as the resonant polarization. The periodic array of QW's is buried in a semi-infinite medium with a

background dielectric constant ϵ_b. The difference of the background dielectric constant between the QW and barrier region is neglected. The effect of the background dielectric on the resonant current density is taken into account by a renormalized radiation Green's function (see the Appendix) as mentioned below.

In order to apply the scheme in Sec. II to the present models, we need to evaluate the resonant energy $E_{\nu 0}$ and radative correction $\tilde{\mathcal{A}}_{\mu 0,0\nu}$ for the matter excitation with $\boldsymbol{k}_\parallel = 0$. Because of the large distance between neighboring layers, the electronic interaction between the layers is safely neglected. In model (A), $E_{\nu 0} = E_{2p,1s}$, i.e., is the $1s$-$2p$ excitation energy corrected by the dipole-dipole interaction energy, and in model (B), it is the lowest QW exciton energy E_{QW} allowed for the lateral polarization. For the evaluation of the dipole-dipole interaction energy and the radiative correction, it is enough to have knowledge of the induced current densities for the excitations of each model system.

The induced current density in the unit cell to be used in model (A) is

$$I^{(x)}_{2p,1s}(\boldsymbol{r}) = \langle \phi_{2p} | \hat{I}_x(\boldsymbol{r}) | \phi_{1s} \rangle, \tag{13}$$

where ϕ_{2p} and ϕ_{1s} are the hydrogen $2p$ and $1s$ eigenfunctions and $\hat{I}_x(\boldsymbol{r})$ is the x component of the current density operator. For a single quantum well of model (B), the current density in the unit cell associated with the excitation of the QW exciton is given as

$$I^{(x)}_{x,0}(\boldsymbol{r}) = A_{QW} \frac{2a_0}{L_{QW}} \sin^2\left(\frac{\pi z}{L_{QW}}\right) I_0, \tag{14}$$

$$I_0 = -\frac{e}{m\Omega^2} \int_\Omega d\bar{\boldsymbol{r}} u_{v,\mathbf{k}_0}(\bar{\boldsymbol{r}}) [p_x u^*_{c,\mathbf{k}_0}(\bar{\boldsymbol{r}})], \tag{15}$$

where A_{QW} represents the amplitude of the exciton relative motion at $\boldsymbol{r}_{e\parallel} = \boldsymbol{r}_{h\parallel}$ in the lateral direction, normalized by the same quantity in the absence of the exciton effect, Ω is the volume of the crystal unit cell, $\sin^2(\pi z/L_{QW})$ represents the envelope functions of the electron and hole for the lowest quantized states, a_0 is the size of the crystal unit cell in the normal direction of QW, L_{QW} is the thickness of a QW, and $u_{j,\mathbf{k}_0}$ is the periodic part of the Bloch function of the jth band at the band edge. We treat A_{QW} as a parameter to describe the intensity of the exciton transition [see Eq. (29)]. In terms of these expressions of the current density, we can give the analytic expressions of the current densities.

For the evaluation of $\tilde{\mathcal{A}}_{\mu 0,0\nu}$ for models (A) and (B), it will be more appropriate, rather than to use the general expressions (2) or (5), to employ the following expression with explicit consideration of the translational symmetry in the lateral direction. The radiative correction is nonzero only among the excitations $\{\mu \to \nu, \sigma \to \tau\}$ with the same lateral wave vector $\bar{\boldsymbol{k}}_\parallel$, and it has the expression as

$$\tilde{\mathcal{A}}_{\mu\nu,\tau\sigma} = \sum_{\mathbf{G}_\parallel} B_{\mu\nu,\tau\sigma}(\bar{\boldsymbol{k}}_\parallel + \boldsymbol{G}_\parallel, \omega), \tag{16}$$

where

$$B_{\mu\nu,\tau\sigma}(\boldsymbol{k}_\parallel, \omega) = \frac{-1}{c^2 s} \int\int dz\, dz'\ \ G^{(1D)}(z,z';\bar{q}) \times \tilde{\boldsymbol{I}}_{\mu\nu}(-\boldsymbol{k}_\parallel, z) \cdot (\mathbf{1} - \hat{\boldsymbol{e}}_{\mathbf{k}} \hat{\boldsymbol{e}}_{\mathbf{k}}) \cdot \tilde{\boldsymbol{I}}_{\tau\sigma}(\boldsymbol{k}_\parallel, z'), \tag{17}$$

with $\boldsymbol{k} = (\boldsymbol{k}_\parallel, \bar{q})$, s is the area of the lateral unit cell, $\boldsymbol{G}_\parallel$ the 2D reciprocal lattice vector, and $\bar{q} = \sqrt{q^2 - k_\parallel^2}$. (For $q^2 < k_\parallel^2$, the branch with $\mathrm{Im}[\bar{q}] > 0$ should be chosen.) The lateral Fourier component of the current density is defined as

$$\tilde{\boldsymbol{I}}_{\tau\sigma}(\boldsymbol{k}_\parallel, z) = \int d\boldsymbol{r}_\parallel \exp(-i\boldsymbol{k}_\parallel \cdot \boldsymbol{r}_\parallel) \boldsymbol{I}_{\tau\sigma}(\boldsymbol{r}_\parallel, z), \tag{18}$$

and the one-dimensional radiation Green's function

$$G^{(1D)}(z,z';\bar{q}) = \frac{-2\pi i}{\bar{q}} \exp(i\bar{q}|z - z'|) \tag{19}$$

is the solution of the equation

$$-\left(\frac{d^2}{dz^2} + \bar{q}^2\right) G^{(1D)}(z,z';\bar{q}) = 4\pi\delta(z - z'). \tag{20}$$

This form of radiative correction is convenient to take the background dielectric into account for model (B). We simply need to replace $G^{(1D)}(z,z';\bar{q})$ with the appropriate one, renormalizing the effect of the background dielectric, as shown below.

A change necessary in applying the nonlocal framework in Sec. II to model (B) is the definition of $\boldsymbol{A}_0$ and the use of the renormalized radiation Green's function in evaluating the radiative correction. This can be seen from the following argument. Since we consider only the $\boldsymbol{k}_\parallel = 0$ state in each QW, the Maxwell equations are reduced to the one-dimensional equation as

$$\left[\frac{d^2}{dz^2} + q^2\{1 + 4\pi\chi_b \Theta_b(z)\}\right] A_x(z,\omega) = -\frac{4\pi}{c} J^{(x)}(z,\omega), \tag{21}$$

$$J^{(x)}(z,\omega) = \int dz'\, \chi^{(1)}(z,z';\omega) A_x(z',\omega), \tag{22}$$

$$\chi^{(1)}(z,z';\omega) = \frac{1}{cs} \sum_{l=1}^{N} \frac{I^{(x)}_{l,0x}(\boldsymbol{k}_\parallel = 0, z) I^{(x)}_{l,x0}(\boldsymbol{k}_\parallel = 0, z')}{E_{QW} - \hbar\omega - i0^+}, \tag{23}$$

where E_{QW} is the energy of the QW exciton, l the layer number, and $I^{(x)}_{l,x0}$ the x component of the current density accompanying the excitation on the lth layer. The step function $\Theta_b(z)$ is 1 (0) inside (outside) the QW's. The effect of $\boldsymbol{G}_\parallel \neq 0$ terms on $\chi^{(1)}$ is neglected. The vector potential $\boldsymbol{A}_0$ is the solution of Eq. (21) in the absence of the resonant current

density $J^{(x)}(z,\omega)$, but in the presence of the background dielectric. Such a field acts on the resonant current density as the ''incident'' field.

The analytic expression of the radiative correction for the x-polarized matter excitation with $\bar{k}_\parallel=0$ is given as follows. Between the different atomic layers $l\neq m$ of model (A), we have

$$\tilde{\mathcal{A}}_{l(2p_x,1s),m(1s,2p_x)}=i\pi\tilde{\mathcal{A}}_{ap}\frac{e^{iq(Z_l-Z_m)}}{q\tilde{q}^8}, \tag{24}$$

where the x axis is parallel to an edge of the square lattice, and

$$\tilde{q}^2=q^2+\alpha^2, \quad \alpha=\frac{3}{2a_B},$$

$$\tilde{\mathcal{A}}_{ap}=\frac{2}{c^2a_B^8}\left(\frac{1}{b}\right)^2\left(\frac{\sqrt{2}\hbar e}{a_Bm}\right)^2,$$

with Bohr radius a_B. The radiative shift and width of a single atomic layer ($l=m$) are given as

$$\mathrm{Re}\tilde{\mathcal{A}}_{l(2p_x,1s),l(1s,2p_x)}=-\pi\tilde{\mathcal{A}}_{ap}\left(\frac{1}{\tilde{q}^8\alpha}+\frac{1}{2\alpha^3\tilde{q}^6}+\frac{3}{8\alpha^5\tilde{q}^4}+\frac{5}{16\alpha^7\tilde{q}^2}\right), \tag{25}$$

$$\mathrm{Im}\tilde{\mathcal{A}}_{l(2p_x,1s),l(1s,2p_x)}=\pi\tilde{\mathcal{A}}_{ap}\frac{1}{q\tilde{q}^8}. \tag{26}$$

The radiative correction of the x-polarized QW exciton with $\bar{k}_\parallel=0$ is calculated in terms of the renormalized Green's function in the Appendix. Its explicit form for a single quantum well ($l=m$) is

$$\tilde{\mathcal{A}}_{l,l}=\tilde{\mathcal{A}}_{QW}\{32i\pi^4(e^{iX}-1)+16i\pi^4\delta e^{2il\tilde{q}L}e^{-2iX}(e^{iX}-1)^2+32\pi^4X-20\pi^2X^3+3X^5\}/\{2\tilde{q}^3(-4\pi^2+X^2)\}, \tag{27}$$

$$X=\bar{q}L_{QW}, \quad \bar{q}=q\sqrt{\epsilon_b}, \quad \delta=\frac{\bar{q}-1}{\bar{q}+1},$$

and between the lth and mth QW's ($l<m$) is

$$\tilde{\mathcal{A}}_{l,m}=\frac{8\pi\tilde{\mathcal{A}}_{QW}ie^{i\tilde{q}(l+m)L}e^{-2iX}(e^{iX}-1)^2(\delta+e^{2i\tilde{q}mL}e^{iX})}{\tilde{q}^3(-4\pi^2+X^2)^2}, \tag{28}$$

where

$$\tilde{\mathcal{A}}_{QW}=\frac{4\pi A_{QW}^2I_0^2S_{QW}}{c^2L_{QW}^2}. \tag{29}$$

This quantity $\tilde{\mathcal{A}}_{QW}$ is treated as a parameter to fit the imaginary part of $\tilde{\mathcal{A}}_{i,i}$ to the experimentally observed radiative width Γ_0.

Once we have evaluated $E_{\nu 0}$ and $\tilde{\mathcal{A}}_{\mu 0,0\nu}$, we can solve $\mathbf{SX}=\mathbf{F}^{(0)}$ for a given incident field, Eq. (11), to obtain $F_{\mu 0}$'s, from which the induced current density, Eq. (7), and then the vector potential, Eq. (10) are calculated. As physical quantities, we calculate the reflection amplitudes in both frequency and time domains for various N, i.e., $r_N(\omega)$ and $\bar{r}_N(t)$, and also the internal field strength as a function of frequency and position.

The reflection amplitude in the frequency domain $r(\omega)$ is obtained from Eq. (10). When applied to the model (A) for x-polarized normally incident light of frequency ω, Eq. (9) gives the vector potential (x component) as

$$A_x(z)=A_0e^{iqz}+\frac{1}{2\pi^2c^2\sqrt{N_0^{(2D)}}}\left(\frac{1}{b}\right)^2\sum_l\int dk_z \times\frac{e^{ik_z(z-Z_l)}\tilde{I}_{l,0x}^{(x)}(\boldsymbol{k}_\parallel=0,k_z)}{k_z^2-(q+i0^+)^2}\frac{F_{l,x0}}{E_{2p,1s}-\hbar\omega-i0^+}, \tag{30}$$

where $F_{l,x0}$ the solution of Eq. (10), with $F_{l,x0}^{(0)}$ defined as

$$F_{l,x0}^{(0)}=\sqrt{N_0^{(2D)}}e^{iqZ_l}\tilde{I}_{l,x0}^{(x)}(\boldsymbol{k}_\parallel=0,q)A_0. \tag{31}$$

The contribution of $I^{(x)}(\boldsymbol{G}_\parallel\neq 0,k_z)$ terms is neglected in Eq. (28).

The reflection amplitude is the ratio $r(\omega)=A_x/A_0$ in the region $z<Z_1$. The integral in Eq. (30) can be evaluated by choosing the appropriate contour in the complex k_z plane. For $z-Z_j<0$, which is the region to define the reflection amplitude, the contribution of the pole $k_z=-q-i0^+$ is taken into account.

The response field of the multiple QW's for normal incidence of light is described in terms of the 1D renormalized Green's function, Eqs. (A2) and (A3), as

$$A_x(z)=A_{0,x}(z)+\frac{1}{c^2}\int dz'\tilde{G}_s(z,z')J^{(x)}(z',\omega) \tag{32}$$

$$=A_{0,x}(z)+\frac{1}{c^2s\sqrt{N_0^{(2D)}}}\int dz'\tilde{G}_s(z,z')\times\sum_l\frac{I_{l,0x}(\boldsymbol{k}_\parallel=0,z')F_l}{E_{QW}-E-i0^+}, \tag{33}$$

where $A_{0,x}$ is the amplitude of the vector potential induced by the field $A_i(z,\omega)$ incident on a semi-infinite ($z>0$) background medium,

$$A_0(z)=A_ie^{iqz}-A_i\delta e^{-iqz} \quad (z\leqslant 0), \tag{34}$$

$$A_0(z)=\frac{2A_i}{1+\sqrt{\epsilon_b}}e^{i\sqrt{\epsilon_b}qz} \quad (z>0). \tag{35}$$

The variables F_l are solutions of the coupled equations (10) for this model, where $F^{(0)}$ has a similar form as Eq. (31) with an appropriate change due to Eqs. (34) and (35). The strength of the response field is defined as $|A_x(z)/A_i|^2$. For $z<0$, it is the reflectivity, and for $z>0$, it gives the internal field, as will be discussed later. The term with $|z-z'|$ dependence in $\tilde{G}_s(z,z')$ plays a crucial role in determining the peculiar form of the internal field.

The reflection amplitude depends on the number of layers, N. For $N=1$ we get an analytic expression in the absence of nonradiative damping ($\gamma=0$) for model (A) as

$$r_1(\omega)=\frac{-i\Gamma_0}{E_{2p,1s}-\hbar\omega-\Delta_0-i\Gamma_0}, \tag{36}$$

assuming that the thickness of the single layer is thin enough, where Γ_0 and $-\Delta_0$ are the radiative width and shift, respectivily, of a single layer in the case of $\boldsymbol{k}_\parallel=0$. If the ω dependence of Γ_0 and Δ_0 is negligible, Eq. (36) gives a simple Lorentzian curve for the reflectivity $|r_1(\omega)|^2$, the peak of which occurs at $E_{2p,1s}-\Delta_0$ ($\Delta_0<0$) with a half width at half maximum (HWHM) of Γ_0 (>0).

For larger N, we generally need a numerical calculation to obtain $r_N(\omega)$. However, if the ω dependence of $\tilde{\mathcal{A}}(\omega)$ is negligible, i.e., if we can replace $\tilde{\mathcal{A}}(\omega)$ with $\tilde{\mathcal{A}}(E_{2p,1s}/\hbar)$, one can analytically solve the coupled equation for $X_{l,x0}$ in general and obtain

$$\tilde{r}_N(\omega)=\frac{-iN\Gamma_0}{E_{2p,1s}-\hbar\omega-\Delta_0-iN\Gamma_0}. \tag{37}$$

This is the same result as that by Ivchenko.[10,29] Though it describes the N-linear growth of the SR mode analytically, its endless growth is unacceptable as mentioned in detail in the Introduction. An essentially same argument holds for model (B) if the background dielectric is assumed to be, not semi-infinite, but infinite, which is the case treated by Ivchenko.

Proper consideration of the ω dependence of the radiative correction leads to the reflectivity with reasonable N dependence.[19] The reflectivity spectra for model (B) are shown in Fig. 2 for (a) $N=2-100$, and (b) $N=100-500$. For the numerical calculation, we take $E_{QW}=1.5152$ eV, $\epsilon_b=12.6$, and $\Gamma_0=0.026$ meV. The width of a quantum well is assumed to be $L_{QW}=8$ nm. Due to the interference with the light reflected by the background, the resonant part is slightly deformed from Lorentzian shape in Fig. 2(a). For larger N in Fig. 2(b), the resonant part is obviously different from Lorentzian shape, but approaches ''silk-hat'' shape, which is typical for a photonic gap. Since the resonant levels of different QW's are electronically isolated, this spectral evolution is entirely caused by the ω and N dependences of the radiative correction, which becomes more and more important as N gets larger. The spectral width (HWHM) extracted from the calculated spectrum is plotted as a function of N in Figs. 3 and 4 for models (A) and (B). For small N, the N-linear dependence of the radiative broadening is seen and it starts to be saturated for $N\sim40$ for model (A) and for $N\sim250$ for model (B).

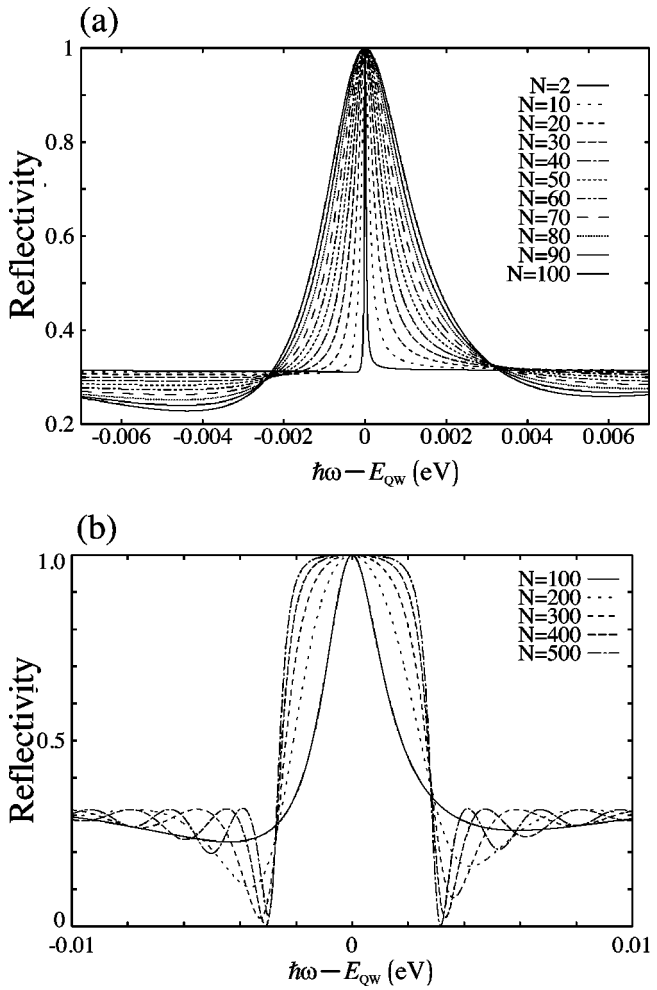

FIG. 2. Reflectivity of Bragg-arranged N QW's. (a) For $N=2-100$, (b) for $N=100-500$.

Since the radiative width is related to the decay of the matter excitation, we have also calculated the temporal response of the N-layer system $I_N(t)$ for an incident Gaussian pulse covering the resonant region,

$$I_N(t)=\left|\int d\omega r_N(\omega)e^{-i\omega t}e^{-(\omega-\omega_0)^2/\sigma^2}\right|^2. \tag{38}$$

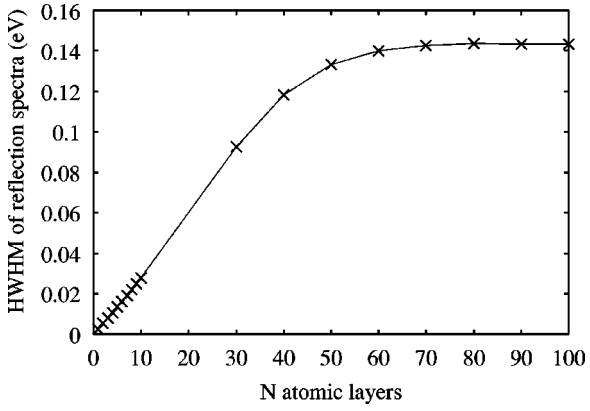

FIG. 3. The radiative width of the spectra for model (A).

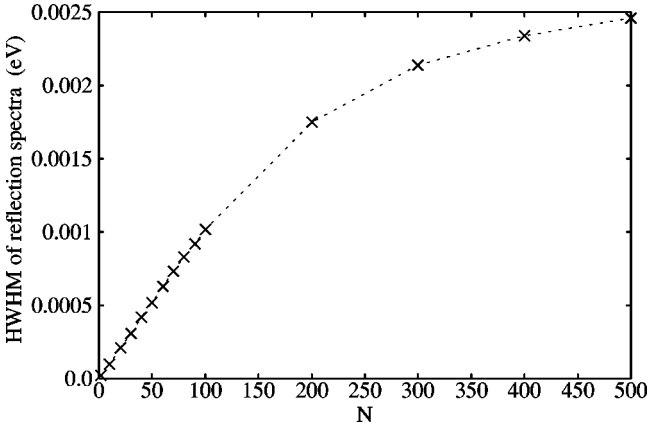

FIG. 4. The radiative width for model (B).

In Fig. 5, we plot the time dependence of the reflected intensity in logarithmic scale $[\log_{10} I_N(t)]$ for (a) $N=2$—100 and (b) $N=100$—500. In Fig. 5(a), except for the initial part due to the quick response of the background dielectric, we see the linear decay behavior, which shows the N-linear growth of the radiative decay rate. For $N \geqslant 200$, Fig. 5(b) shows the slower decay for larger N, in addition to the appearance of oscillations. The oscillation period reflects the width of the silk-hat in the reflectance spectrum. Essentially same behavior is obtained for model (A), too. From the N dependence of the reflectivity in ω and t domains, we may conclude that the SR mode begins to lose its meaning when N becomes so large that the reflectivity spectrum begins to be distorted from a Lorentzian shape.

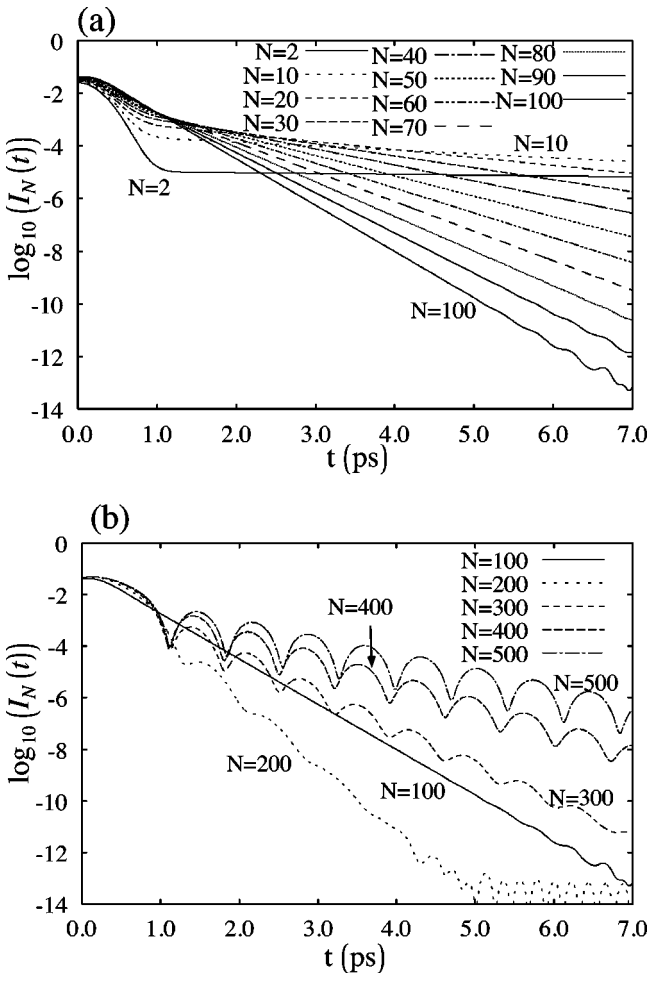

FIG. 5. Time-resolved reflection dynamics for a Gaussian pulse of light on the periodic structures containing N QW's. $\sigma=3$ meV. (a) For $N=2\sim-100$, (b) for $N=100\sim-500$.

IV. DISPERSION EQUATION FOR RESONANT PHOTONIC CRYSTALS

Applying the SS mode condition $\det|\mathbf{S}|=0$ to an arbitrary 3D crystal with various resonant excitations, one of the present authors derived a general dispersion equation of the EM field in such a medium.[25] Especially, the equation was put in a form directly comparable with the scheme of x-ray dynamical scattering.[31] Though this result can be applicable to the present problem, we will give a simpler argument here.

If we consider a periodic matter system with a single resonant level in each unit cell, the eigenstate is characterized by the wave vector of the lattice, and for each wave vector there is only one eigenstate. (The present system of the $N=\infty$ Bragg reflector is an example of such matter systems.) Then, $\det|\mathbf{S}|$ is factorized into the product of 1×1 matrices for each $\boldsymbol{k}$. Thus, the dispersion equation for a given $\boldsymbol{k}$ is

$$0=E_{\mathbf{k}}-\hbar\omega+\tilde{\mathcal{A}}_{\mathbf{k}0,0\mathbf{k}}(\omega), \tag{39}$$

where $\tilde{\mathcal{A}}_{\mathbf{k}0,0\mathbf{k}}(\omega)$ is the radiative correction calculated for the resonant level with the wave vector $\boldsymbol{k}$.

According to the Fourier representation of the radiative correction (5), we need to calculate the Fourier transform of the induced current density of the matter excitation. For the excitation characterized by the wave vector $\bar{\boldsymbol{k}}$, the Fourier component of its current density is given as

$$\tilde{\boldsymbol{j}}_{\bar{\mathbf{k}}}(\boldsymbol{k})=\sqrt{N_0}\,\delta_{\bar{\mathbf{k}}-\mathbf{k}-\mathbf{G}}\tilde{\boldsymbol{j}}^{(0)}(\boldsymbol{k}), \tag{40}$$

where $\tilde{\boldsymbol{j}}^{(0)}(\boldsymbol{k})$ is the Fourier component of the lattice periodic part of the current density and $\boldsymbol{G}$ is a reciprocal lattice vector. The number of the lattice points, N_0, is put $\rightarrow\infty$ at the last stage of the calculation. The two Kronecker delta's appearing in the expression of the radiative correction (5) are rewritten as

$$\delta_{\bar{\mathbf{k}}-\mathbf{k}-\mathbf{G}}\delta_{\bar{\mathbf{k}}-\mathbf{k}-\mathbf{G}'}=\delta_{\mathbf{G},\mathbf{G}'}\frac{8\pi^3}{\Omega N_0}\delta(\bar{\boldsymbol{k}}-\boldsymbol{k}-\boldsymbol{G}) \tag{41}$$

in terms of a delta function and the volume Ω of the unit cell. This allows us to rewrite the radiative correction as

$$\tilde{\mathcal{A}}_{\bar{\mathbf{k}}0,0\bar{\mathbf{k}}}(\omega)=-\frac{4\pi}{\Omega c^2}\sum_{\mathbf{G}}\frac{|\boldsymbol{S}(\bar{\boldsymbol{k}}+\boldsymbol{G})|^2}{(\bar{\boldsymbol{k}}+\boldsymbol{G})^2-(q+i0^+)^2}, \tag{42}$$

where $\boldsymbol{S}(\boldsymbol{k})$ is the transverse component ($\perp\boldsymbol{k}$) of the current density $\tilde{\boldsymbol{j}}^{(0)}(\boldsymbol{k})$.

Inserting this form of $cal\tilde{A}$ into Eq. (39), we obtain the dispersion equation of this periodic system. This dispersion equation is valid for any dimension, as long as the number of

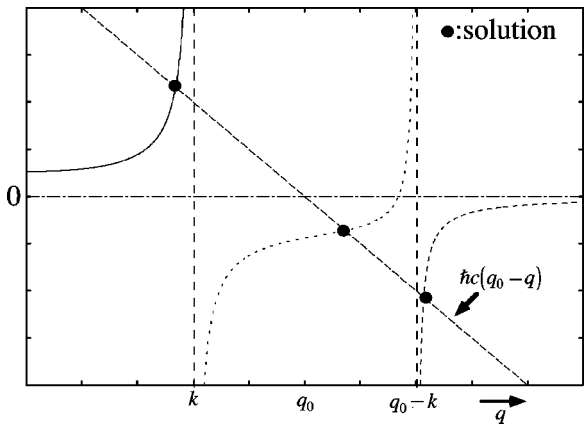

FIG. 6. Graphic solution of the dispersion equation for a given k. The crossing points of the curves and the straight line gives the eigenfrequencies.

the resonant level is 1. For the lattice of model (A) as an example of a 1D resonant Bragg reflector, which has largely different lattice constants in the lateral and normal directions ($b \ll d$), we may consider only those reciprocal lattice vectors in the normal direction in order to discuss the dispersion curves near the lowest-gap region. Thus we put $\overline{\boldsymbol{k}}=(\overline{\boldsymbol{k}_{\parallel}}=0,k)$ and $\boldsymbol{G}=(\boldsymbol{G}_{\parallel}=0,g)$, where $g=g_l=2l\pi/d$ ($l=0,\pm 1,\pm 2,\pm 3,\ldots$). The k dependence of the resonant energy, $E(k)$, is negligible, so that we put $E(k)=\hbar\omega_0$. The Bragg condition $d=\lambda_0/2$ is rewritten as $d=\pi c/\omega_0$ or $g_1/2=\omega_0/c$ (= the boundary of the first Brillouin zone).

Denoting ω_0/c as q_0, we obtain the dispersion equation of the resonant photonic crystal as

$$\hbar c(q_0-q)=\frac{|S(0)|^2}{k^2-q^2}+\sum_{l=1}^{\infty}|S(2lq_0)|^2 \times\left\{\frac{1}{(k+2lq_0)^2-q^2}+\frac{1}{(k-2lq_0)^2-q^2}\right\}. \tag{43}$$

The solution $q=q(k)$ of this equation gives the dispersion relation of the EM wave in this resonant photonic crystal. The form of this equation allows us to solve it graphically as shown in Fig. 6, where the right- and left-hand sides of Eq. (43) are drawn as functions of $q(=\omega/c)$ in the neighborhood of the lowest photonic gap. The crossing points (solid circle) are the solutions with real k and ω. Obviously, there are three real roots in this frequency region. The gap mode has a very weak dispersion, and its frequency is slightly above ω_0.

For the lattice of the two-level atoms ($1s$-$2p$ transition of hydrogen atoms), we derive the Fourier coefficients

$$S(2lq_0)=\frac{4\pi}{\Omega_0 c^3}\left(\frac{\sqrt{2}\hbar e}{a_B m}\right)^2\frac{1}{\left[\left(\frac{3}{2}\right)^2+a_B^2(k+2lq_0)^2\right]^2}, \tag{44}$$

with $l=0,\pm 1,\pm 2,\ldots,\ \Omega_0=b^2 d$.

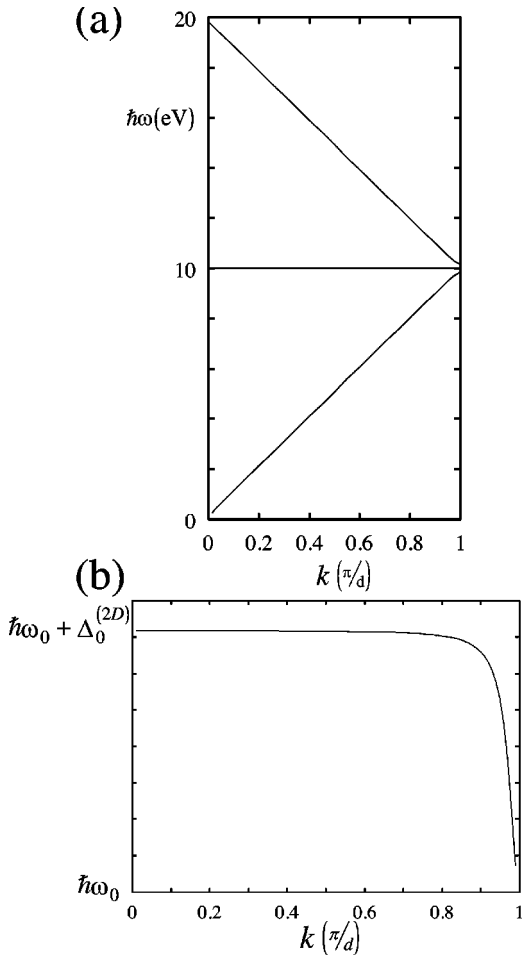

FIG. 7. (a) Dispersion curves obtained from the method of Fig. 6. (b) The gap mode dispersion in an enlarged scale.

Solving Eq. (43) numerically, we obtain the dispersion curves near the lowest photonic gap as in Fig. 7, which is in contrast with the result derived from Eq. (1) for $\gamma=0$ and $d=\pi/q_0$. Namely, the gap mode with very flat dispersion appears in the present treatment, while it is missing in the dispersion based on Eq. (1). The gap mode has a very weak dispersion and its frequency range is between ω_0 and $\omega_0+|\Delta_0|$, where $\hbar|\Delta_0|$ is the radiative shift of the single-layer excitation with $\boldsymbol{k}_{\parallel}=0$. Since the present method takes complete account of radiative interaction, the difference was believed to be due to the incompleteness of Eq. (1). The reason has turned out[24] to be due to the neglect of the radiative shift term in the denominator of Eq. (1) in discussing the form of the dispersion curve by the authors of the litereature,[28,30] though its presence was formally noted by Ivchenko.[10,29] Adding a radiative shift term in the denominator of Eq. (1), we could numerically reproduce a very similar gap mode branch. However, in view of our recent result mentioned in the Introduction[24] that Ivchenko's scheme and ours are analytically equivalent only in the limit of thin layers, we will need a further study to clarify the equivalence with respect to the photonic band dispersion.

The magnitude of the photonic band gap is equal to $E_{gap}=2\sqrt{2\hbar\omega_0\Gamma_0/\pi}$, which is also the case for the disper-

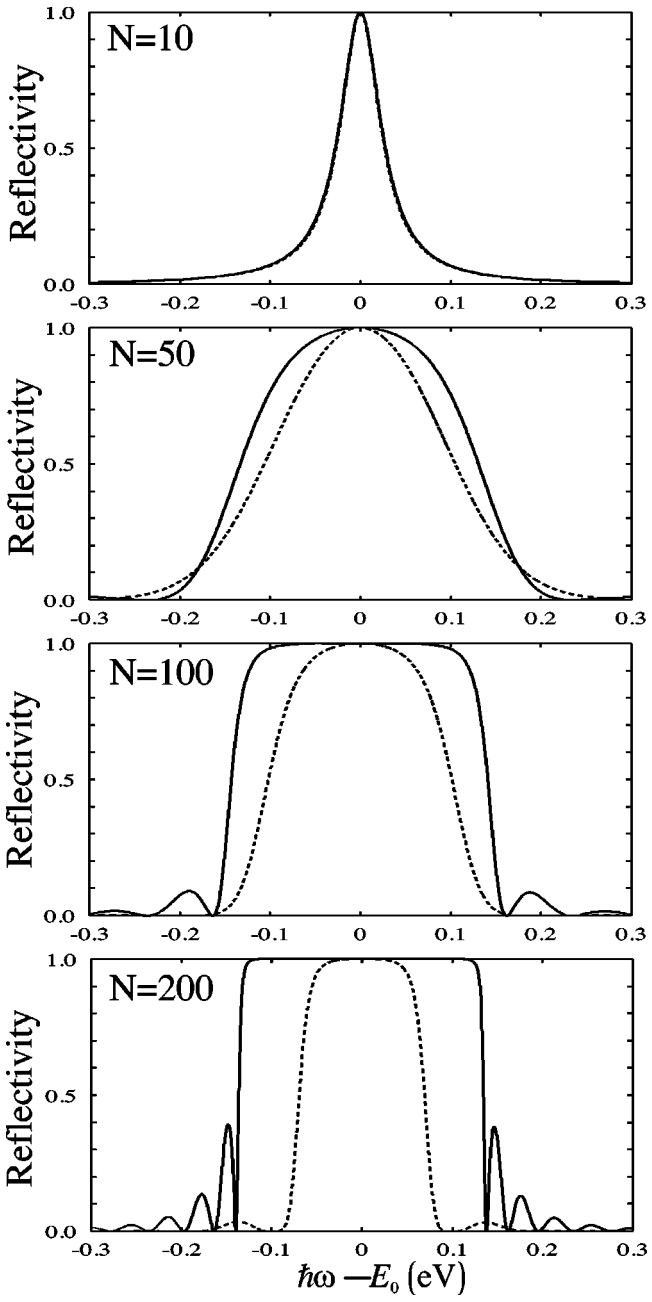

FIG. 8. Comparison of reflectivity spectra. Dashes lines are due to the SR mode alone. Solid lines contain the effect of all modes.

sion relation derived from Eq. (3).[30] This value agrees well with the width of the silk-hat in the calculated reflectivity spectrum for large N.

V. DISCUSSION AND SUMMARY

A. Contribution of the SR mode alone

Among the various excited states of the atomic layers, the SR mode is the linear combination of single-layer excitations with alternating sign from layer to layer, i.e., the state with $k_z=\pi/d$. If we neglect all other states in calculating the optical response, the reflectivity has the forms in Fig. 8 for various N. The evolution from a Lorentzian to silk-hat shape

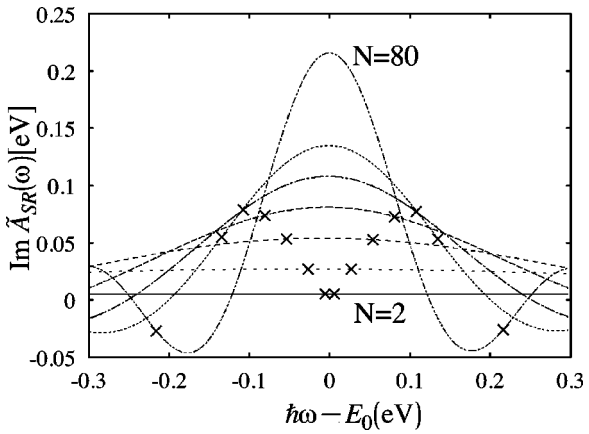

FIG. 9. The ω dependence of $\mathrm{Im}\tilde{\mathcal{A}}_{SR}^{N}(\omega)$ for $N=2,5,10,20,30,40,50,80$. Crosses on each curve are ω's for $\hbar\omega=E_0\pm\mathrm{Im}\tilde{\mathcal{A}}_{SR}(E_0/\hbar)$.

is reproduced, but the width of the silk-hat is smaller than the corresponding curve in Fig. 2, and it tends to be zero as $N\to\infty$. This means that the states which form the photonic gap are not simply made of the SR mode. We need the contribution of other states with $k_z\neq\pi/d$ to realize the full photonic gap. Thus, in the photonic band regime (large N), all the excited states of the Bragg reflector are rearranged to form photonic band states above and below the photonic gap, and the states contributing to the gap mode.

The reflectivity in this case is written as

$$|r_{SR}^{(N)}(\omega)|^2=\left|\frac{N\Gamma_0}{E_0-\hbar\omega+\tilde{\mathcal{A}}_{SR}^{(N)}(\omega)}\right|^2, \tag{45}$$

so that the spectral evolution is solely described by the radiative correction $\tilde{\mathcal{A}}_{SR}^{(N)}(\omega)$. The ω and N dependence of this quantity is shown in Fig. 9. The crosses in Fig. 9 represent $\hbar\omega$'s for $\hbar\omega=E_0\pm\mathrm{Im}\tilde{\mathcal{A}}_{SR}(E_0/\hbar)$. If a curve is flat enough between the two crosses, the ω dependence of $\tilde{\mathcal{A}}_{SR}(\omega)$ may be negligible. This is the explicit demonstration of our main conclusion that the ω dependence of $\tilde{\mathcal{A}}_{SR}^{(N)}$ determines the two regimes. Namely, for small N the ω dependence is negligible and $\tilde{\mathcal{A}}_{SR}^{(N)}(\omega)\sim\tilde{\mathcal{A}}_{SR}^{(N)}(\omega_0)=-iN\mathrm{Im}[\tilde{\mathcal{A}}_{SR}^{(1)}(\omega_0)]$, leading to the formation of the SR mode. For large N, the ω dependence is quite important, which leads to the photonic band regime.

B. Evidence of a gap mode

In Sec. IV we have derived a gap mode in the photonic band structure of a resonant Bragg reflector. The gap mode should manifest itself in appropriate measurements. For example, the reflectance spectrum of a photonic crystal should have a dip in the spectral range of total reflection, in view of the real (k,ω) dispersion of the gap mode allowing the propagation of EM waves in this narrow frequancy range.

Evidence of the gap mode can be seen in the nonlocally calculated reflectance spectra of finite-N systems. Figure 10 shows such an example. If we expand the energy scale very

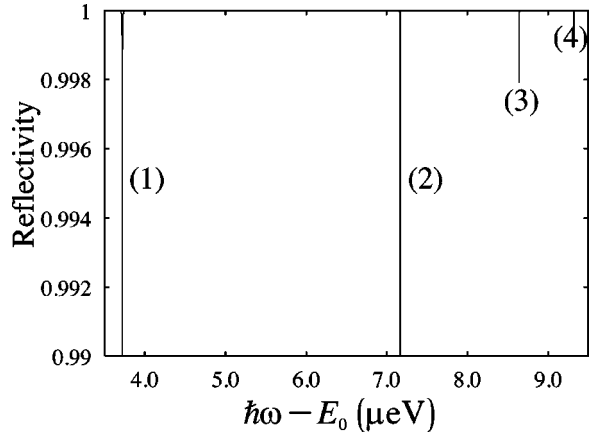

FIG. 10. Evidence of the size-quantized gap modes for $N=101$. For any $N(\geqslant 2)$, there occur such fine dips in the region of total reflection.

much, we can find very narrow dips on the top part (total reflection range) of the Lorentzian or silk-hat-shaped reflectance curves for finite N. They are, so to speak, the size-quantized levels of the gap mode or, in other word, the very weakly optically active non-SR modes of the system buried in the middle of the broad SR mode or developing photonic gap. Since there are one SR mode and $(N-1)$ non-SR mode in a small-N system, the number of such narrow dis is $(N-1)$. In the limit of a photonic crystal $(N=\infty)$, such dips should merge into a broader dip.[24]

More positive evidence for the gap mode with real k is obtained by calculating the internal field for the frequencies of the very sharp dips mentioned above. Figure 11 shows the internal field patterns for these particular frequencies. It is remarkable that they have standing-wave patterns. For frequencies outside the sharp dips, the internal field has a simple evanescent pattern, reflecting the total reflection range. Since the calculations of the reflectance spectrum and internal field patterns are made independently from that of the photonic band dispersion, the emergence of the sharp dips and their standing-wave character strongly supports the existence of the propagating mode in the photonic gap.

C. Upper limit of the speedup effect

We have studied the behavior of 1D resonant Bragg reflectors as a function of the layer number N. Our results show that the concept of the SR mode and/or speedup effect, characterizing the peculiarity of the system for small N, has a validity limit. The limit can be obtained from the detailed study of $\tilde{\mathcal{A}}_{SR}^{(N)}(\omega)$ as in Fig. 9, but a simple criterion will be that $N\Gamma_0$ should be much smaller than half a photonic gap, i.e., $E_{gap}/2\Gamma_0 \gg N$. In this range of N, the reflectivity spectrum has a Lorentzian shape with its width $N\Gamma_0$, and the decay rate of the reflectivity for an incident Gaussian pulse is $N\Gamma_0/\hbar$. The criterion mentioned above is expected to be applicable to any resonant Bragg reflectors. Namely, if one measures the N dependence of reflectivity, its radiative width or the speedup effect of the radiative decay rate begins to be saturated when N becomes an appreciable fraction of $N_c \equiv E_{gap}/2\Gamma_0$.

We have estimated N_c for the two models in this paper. The values of N_c turn out to be 50 and 190 for models (A) and (B), respectively. The value $N_c=50$ is consistent with the $|r_N(\omega)|^2$ in Ref. 19 or Fig. 3; i.e., the linear growth starts

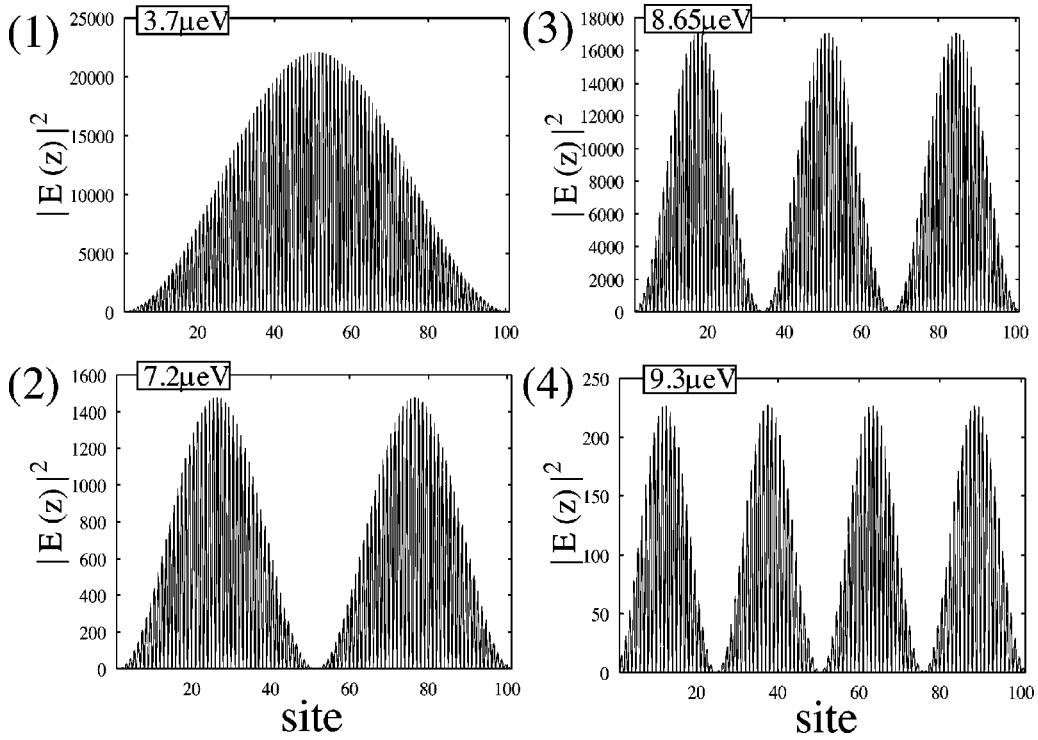

FIG. 11. Internal field patterns at the energies of the sharp dips in Fig. 10

to be saturated at $N\sim 30$ for model (A). The value $N_c=190$ is consistent with the experiment by Hübner *et al.*,[8] where N-linear growth of the radiative width is confirmed for samples of $N\leqslant 100$. Their samples belong to the SR mode regime. One needs to use samples with $N\geqslant 190$ to see the effects of the photonic band regime in this system of multiple QW's. The case of $^{57}FeBO_3$ crystal needs an additional consideration, because (i) the resonance is not electric dipole type and (ii) the resonant wavelength is smaller than the lattice constant. Though the upper limit of speedup certainly exists in this case too, the estimate of Γ_0 for a single layer needs extra work, which will be published elsewhere.

D. Conclusion

In conclusion, we have studied the evolution of the superradiant mode as a function of size N, applying the microscopic nonlocal theory, which takes explicit account of the ω-dependent radiative shift and width from first principles, to the two models of resonant Bragg reflectors. For N comparable to or larger than $E_{gap}/2\Gamma_0$, the ω dependence of the radiative width becomes important, invalidating the concept of the SR mode and leading to the deformation of the Lorentzian spectrum and the temporal response with the N-linear decay constant. A consistent picture has been provided for the evolution from the SR mode regime to the photonic band regime. We have derived the photonic band dispersion for $N\rightarrow\infty$, $\gamma=0$, and $d=\pi/q_0$, which, in contrast to the existing literature, contains a flat gap mode just above ω_0. Evidence of the gap mode has been discussed as very sharp dips in the reflectivity spectrum and their standing-wave patterns of internal field.

ACKNOWLEDGMENTS

The authors are grateful to Professor H. Ishihara and Dr. H. Ajiki for their useful discussions. We thank T. Hirai for showing us his result about the photonic band dispersion and its reflectivity of a resonant Bragg reflector in microscopic and macroscopic schemes. This work was supported in part by a Grant-in-Aid for COE Research (10CE2004) of the Ministry of Education, Culture, Sports, Science and Technology of Japan.

APPENDIX: RENORMALIZED RADIATION GREEN'S FUNCTION

Here we present the explicit form of the renormalized radiation Green's function for a semi-infinite medium with dielectric constant $\epsilon_b(=1+4\pi\chi_b)$. For the normal incidence ($\|z$ axis) of a polarized light along the x axis, we only need to consider the x component of the current density, $J^{(x)}(z)$, which depends only on z. The renormalized Green's function for $\bar{k}_\|=0$ is the solution of the equation

$$\frac{d^2G_s(z,z')}{dz^2}+q^2\{1+4\pi\chi_b\Theta(z)\}G_s(z,z')=-4\pi\delta(z-z'), \tag{A1}$$

where the medium specified by χ_b fills the space $z\geqslant 0$, i.e.,

$$\Theta(z)=\begin{cases}1 & (z\geqslant 0),\\ 0 & (z<0).\end{cases}$$

Assuming the source plane in the semi-infinite medium, i.e., $z'>0$, we obtain the solution of Eq. (A1) as

$$G_s(z,z')=\frac{4\pi i}{\bar{q}+q}e^{i\bar{q}z'}e^{-iqz}\quad (z\geqslant 0), \tag{A2}$$

$$G_s(z,z')=\frac{2\pi i}{\bar{q}}[\,\delta e^{i\bar{q}z'}e^{i\bar{q}z}+e^{i\bar{q}|z-z'|}]\quad (z<0), \tag{A3}$$

where $\bar{q}=q\sqrt{\epsilon_b}$ and $\delta=(\bar{q}-q)/(\bar{q}+q)$. In terms of this $G_s(z,z')$, the solution of Eq. (21) is given as

$$A_x(z)=A_0(z)+\frac{1}{c}\int dz G_s(z,z')J^{(x)}(z',\omega), \tag{A4}$$

where A_0 is the solution of

$$\frac{d^2}{dz^2}A_0(z)+q^2\{1+4\pi\chi_b\Theta(z)\}A_0(z)=0. \tag{A5}$$

*Electronic address: ikawa@aria. mp. es. osaka-u. ac. jp
†Electronic address: cho@mp. es. osaka-u. ac. jp

[1] M. Orrit, C. Aslangul, and P. Kottis, Phys. Rev. B **25**, 7263 (1982).
[2] F. Tassone, F. Bassani, and L.C. Andreani, Nuovo Cimento D **12**, 1673 (1990); **14**, 1156 (1992).
[3] Y. Ohfuti and K. Cho, Phys. Rev. B **51**, 14379 (1995).
[4] U. van Bürck, R.L. Mössbauer, E. Gerdau, R. Rüffer, R. Hollatz, G.V. Smirnov, and J.P. Hannon, Phys. Rev. Lett. **59**, 355 (1987).
[5] M. Hübner, J. Kuhl, T. Stroucken, A. Knorr, S.W. Koch, R. Hey, and K. Ploog, Phys. Rev. Lett. **76**, 4199 (1996).
[6] M. Hübner, J. Kuhl, S. Haas, T. Stoucken, S.W. Koch, R. Hey, and K. Ploog, Solid State Commun. **105**, 105 (1998).
[7] Y. Merle d'Aubigné, A. Wasiela, H. Mariette, and T. Dietl, Phys. Rev. B **54**, 14003 (1996).
[8] M. Hübner, J.P. Prineas, C. Ell, P. Brick, E.S. Lee, G. Khitrova, H.M. Gibbs, and S.W. Koch, Phys. Rev. Lett. **83**, 2841 (1999).
[9] J.P. Prineas, C. Ell, E.S. Lee, G. Khitrova, H.M. Gibbs, and S.W. Koch, Phys. Rev. B **61**, 13 863 (2000).
[10] E.L. Ivchenko, A.I. Nesvizhskii, and S. Jorda, Fiz. Tverd. Tela (St. Petersburg) **36**, 2118 (1994) [Phys. Solid State **36**, 1156 (1994)].
[11] T. Stroucken, A. Knorr, P. Thomas, and S.W. Koch, Phys. Rev. B **53**, 2026 (1996).
[12] L.C Andreani, G. Panzarini, A.V. Kavokin, and M.R. Vladimirova, Phys. Rev. B **57**, 4670 (1998).
[13] J.J. Baumberg, A.P. Heberle, A.V. Kavokin, M.R. Vladimirova, and K. Köhler, Phys. Rev. Lett. **80**, 3567 (1998).
[14] A.V. Kavokin and J.J. Baumberg, Phys. Rev. B **57**, R12 697 (1998).
[15] K. Cho, Suppl. Prog. Theor. Phys. **106**, 225 (1991).
[16] K. Cho, J. Phys. Soc. Jpn. **55**, 4113 (1986).
[17] K. Cho and T. Arakawa, Mater. Sci. Eng., B **48**, 71 (1997).
[18] K. Cho and T. Ikawa, Phys. Status Solidi B **215**, 281 (1999).

[19] T. Ikawa and K. Cho, in *Proceedings of the 25th International Conference on Physics of Semiconductors, Osaka, Japan, 2000*, edited by N. Miura and T. Ando (Springer-Verlag, Berlin, 2001), p. 1731.
[20] L.C. Andreani, F. Tassone, and F. Bassani, Solid State Commun. **77**, 641 (1991).
[21] D.S. Citrin, Solid State Commun. **84**, 281 (1992).
[22] T. Ikawa and K. Cho, J. Lumin. **87-89**, 305 (2000).
[23] T. Ikawa and K. Cho, Physica E (Amsterdam) **13**, 463 (2002).
[24] K. Cho, T. Hirai, and T. Ikawa, J. Lumin. (to be published).
[25] K. Cho, J. Phys. Soc. Jpn. **66**, 2496 (1997).
[26] K. Cho, Mol. Cryst. Liq. Cryst. Sci. Technol., Sect. A **314**, 179 (1998).
[27] K. Cho, J. Lumin. **87-89**, 7 (2000).
[28] I.H. Deutsch, R.J.C. Spreeuw, S.L. Rolston, and W.D. Phillips, Phys. Rev. A **52**, 1394 (1995).
[29] E.L. Ivchenko, Fiz. Tverd Tela (St. Petersburg) **33**, 2388 (1991) [Phys. Solid State **33**, 1344 (1991)].
[30] L.I. Deych and A.A. Lisyansky, Phys. Rev. B **62**, 4242 (2000).
[31] B.W. Batterman and H. Cole, Rev. Mod. Phys. **36**, 681 (1964).
[32] K. Cho and T. Ikawa, Phys. Status Solidi A **190**, 401 (2002).
[33] The sign of the $\tilde{\mathcal{A}}$ terms in the equations for $\{F_{\mu\nu}\}$ is taken as plus, because of the minus sign in the definition of $\tilde{\mathcal{A}}$ in Eq. (2). This choice of sign is physically more reasonable. Though the equations look different from those we used befoere, there is no change mathematically.